Linear model predictive control for glucose regulation in type 1 diabetes patients

Jorge Bonekamp (4474554), Dylan Kalisvaart (4466748)

***Abstract*—This paper presents a linear model predictive control (MPC) strategy for intravenous glucose regulation in patients with type 1 diabetes. The glucoregulatory dynamics for these patients are characterized by large time delays, making MPC an interesting control strategy. A nonlinear glucose model proposed in [7] is linearized and discretized. A linear state-measurement MPC strategy is designed and it is shown that asymptotic stability can be guaranteed for the origin of the closed-loop linearized system. Through simulations in MATLAB with the CVX package, it is shown that the proposed MPC strategy is able to reject glucose level disturbances properly for the linear model and (after correction) for the nonlinear model. The effect of the horizon length, weighting matrices and output-measurement MPC is discussed and MPC is compared to PI-control. Future research could focus on the implementation of linear MPC for glucose level control in type 2 diabetes patients.**

I. Introduction

A. Type 1 diabetes and control approaches

Patients diagnosed with type 1 diabetes suffer from below average insulin production levels [1]. Insulin is a hormone, used in the regulation of glucose. Due to the low insulin levels in diabetes patients, glucose levels in blood (intravenous) may become (and stay) dangerously high after a meal (hyperglycemia, or 'sugar rush' in popular terms). In the worst case, this could lead to (potentially lethal) acidification of the blood (ketoacidosis) [2].

To reduce high intravenous glucose levels, diabetes patients must inject additional insulin before having a meal. A problem with this approach is that patients may inject too much insulin or may not eat enough [1], [2]. Due to the slow dynamics of the glucoregulatory system, the effects become noticeable only after a time delay of 15 minutes, after which it may already be too late for compensation. This results in dangerously low glucose levels some time after the meal (hypoglycemia, or 'sugar crash' in popular terms), which can (in extreme cases) lead to a coma [3].

The response of the intravenous glucose level after a meal without additional insulin injections is characterized by a steady-state ('safe') glucose level of approximately 6 mmol/L and a phase of dangerously high hyperglycemia, possibly followed by a phase of low hypoglycemia. By injecting insulin, the amplitude of the glucose peak during hyperglycemia will be reduced, but the amplitude during hypoglycemia increases. Finding an insulin injection strategy such that the glucose level is regulated back to its steady-state value in a safe way is therefore an important control problem.

Multiple control approaches for insulin infusion have been proposed in literature. A well-studied approach is (fuzzy-) PID control [4]-[6]. There are, however, many problems with PID control. First of all, it cannot handle operational constraints. After tuning the controller, it must be verified *a posteriori* if constraints have not been violated. Furthermore, PID control is hindered by the time delay that is inherent to the glucoregulatory system. As a PID controller makes use of the current error measurement only, non-optimal control actions are applied, because the effect of the applied control action becomes visible in the output only after 15 minutes. Lastly, the frequency at which the intravenous glucose level is measured is often quite low. The applied control action, and as a result the performance, is therefore generally not optimal.

These problems of PID control can be circumvented by the use of model predictive control (MPC). As accurate models of the glucoregulatory system and the effect of meals have been studied [7], [8], MPC is a particularly attractive control approach. It can handle operational constraints and can compute optimal control inputs, taking the time delay of the system and the low sampling frequency into account.

In [8], a nonlinear model predictive control algorithm is proposed. It is claimed that using linear MPC on a linearized model is undesirable, due to the importance of nonlinear effects of the human body that become apparent during hyper- and hypoglycemia. In particular, the human body will shut down processes for very high or very low intravenous glucose levels, to aid in regulating the glucose level back to 6 mmol/L. By linearizing the model, this behavior is lost. The approach of [8] is successful, but the inclusion of a parameter estimation algorithm is needed, which makes the proposed algorithm complex and computationally intensive.

In this paper, a model predictive control strategy is proposed, based on a linearization of the glucose model in [8]. As mentioned in the previous paragraph, linearizing the model results in the loss of restorative effects of the human body. As these effects aid in regulating the glucose level, the system performance will degrade due to linearization. The proposed control actions by linear MPC may therefore be too aggressive for the nonlinear system. The objective of this research is to design and implement a MPC strategy for the linearized model (*in silico*) and to then verify if the computed control action sequence (or a corrected variant) satisfies the performance bounds for the nonlinear system of [8]. Furthermore, the performance of the MPC controlled system is compared to the performance of the system with a PI controller, to see if MPC can be beneficial for this application.

Bonekamp, J. and Kalisvaart, D are master students at DCSC TU Delft, The Netherlands. E-mail addresses: {j.w.bonekamp, d.kalisvaart}@student.tudelft.nl.

The paper is structured as follows. In the rest of this section, a nonlinear continuous-time model of the glucoregulatory system is proposed, which is then linearized and discretized. In Section II, a MPC approach is formulated for the linear system. A state-meaurement MPC approach will initially be proposed and an observer will be added, as in general only the intravenous glucose level is measured. In Section III, proofs will be provided that show asymptotic stability of the closed-loop linearized system. In Section IV, the performance of the closed-loop system will be assessed through simulation in MATLAB with the CVX package and comparisons between MPC and PI control are made. In Section V, the main findings of the research are summarized and recommendations for future research are made.

B. Model

An eight-order nonlinear continuous-time state-space model describing the glucoregulatory system of type 1 diabetes patients can be formulated as follows [7], [8]:

$$\begin{cases} \dot{Q}_1(t) = -F_{01}^c - x_1(t)Q_1(t) + k_{12}Q_2(t) \cdots \\ \quad \cdots - F_R + U_G(t) + EGP_0(1 - x_3(t)) \\ \dot{Q}_2(t) = x_1(t)Q_1(t) - (k_{12} + x_2(t))Q_2(t) \\ \dot{S}_1(t) = u(t) - \frac{S_1(t)}{t_{max,I}} \\ \dot{S}_2(t) = \frac{S_1(t)}{t_{max,I}} - \frac{S_2(t)}{t_{max,I}} \\ \dot{I}(t) = \frac{U_I(t)}{V_I} - k_e I(t) \\ \dot{x}_1(t) = -k_{a1}x_1(t) + k_{b1}I(t) \\ \dot{x}_2(t) = -k_{a2}x_1(t) + k_{b2}I(t) \\ \dot{x}_3(t) = -k_{a3}x_1(t) + k_{b3}I(t) \\ y(t) = h(x,u) = Q_1(t)/V_G \end{cases} \tag{1}$$

Note that the time t in Equation (1) is given in minutes.

For the precise derivation of the model, based on conservation laws, and an overview of model parameters, [7] and [8] can be consulted. We briefly summarize the most important terms in the model. Q_1 represents the mass of intravenous glucose. When divided by the glucose distribution volume V_G, the intravenous glucose concentration y is found. This is the system output, and it is generally the only measured quantity. The affine terms F_{01}^c and F_R represent nonlinear effects of the human body (represented by if-then rules), that are active in case of distress.

Injected insulin is represented by the nonnegative input $u(t)$, which enters a two-compartment system (S_1, S_2) representing the absorption dynamics. In this paper, it is assumed that small glucagon injections (which have an opposite effect from insulin by freeing stored sugars, as modeled in [9]) are allowed and that these injections follow the same dynamics as insulin injections. As a result, $u(t)$ may take on slightly negative values as well. Note that in reality, the dynamics of glucagon are much slower than insulin dynamics [9], which makes this a questionable assumption.

The mass of extravenous glucose (e.g. in muscles) is represented by Q_2. The insulin concentration in blood plasma is described by I. Lastly, the effects of insulin on glucose transport, disposal and endogenous glucose production are described by x_1, x_2 and x_3, respectively.

A meal is modeled by a known disturbance U_G of the form:

$$U_G(t) = \frac{D_G A_G (t - t_0) e^{-(t-t_0)/t_{max,G}}}{t_{max,G}^2} \tag{2}$$

In Equation (2), the mass of glucose in the meal (in grams) is given by D_G and the time at which the disturbance starts is given by t_0. In this paper, it is assumed that D_G and t_0 are known in advance (as was done in [8]), which means the disturbance profile $U_G(t)$ is completely known to the MPC controller. As patients can indicate when they will have a meal and how much sugar is approximately contained in the meal, this can be considered a realistic assumption.

This nonlinear model is then linearized. By linearizing the model, the affine terms $-F_{01}^c$, $-F_R$ and EGP_0 will disappear from Equation (1). While these could be implemented as additional disturbance inputs, it was chosen not to do so. Including these terms, some of which are given by if-then rules, will result in a non-convex optimal control problem. This increases computational complexity and no guarantee can be given that the found solution corresponds to a global optimum. By leaving out these terms, the response of the linearized model will be more violent, which results in more aggressive control action. If needed, the control action can be corrected *a posteriori* to ensure sufficient performance on the nonlinear model. Hence, these affine terms were not included in the linearized model.

The system can therefore be linearized using the equations $A = \frac{\partial f(x,u)}{\partial x}|_{(\bar{x},0)}$, $B = \frac{\partial f(x,u)}{\partial u}|_{(\bar{x},0)}$, $B_d = \frac{\partial f(x,u)}{\partial U_d}|_{(\bar{x},0)}$, $C = \frac{\partial h(x,u)}{\partial x}|_{(\bar{x},0)}$ and $D = \frac{\partial h(x,u)}{\partial u}|_{(\bar{x},0)}$. Note that the equilibria of the nonlinear system (1) are not necessarily relevant if used as operating points in the linearization, due to the disappearance of the affine terms. The operating point $\bar{x}$ was therefore chosen through simulation, in such a way that the resulting linearized system is stable and such that behavior of the linearized system closely matches the behavior of the nonlinear system for a range of small inputs. In this way, the operating point $\bar{x} = [0.70, 0.30, 0, 0, 0, 0.025, 0.030, 0]^T$ was obtained. The state-space description of the linearized system is given by:

$$\begin{cases} \dot{x} = Ax + Bu + B_d U_G \\ y = Cx + Du \end{cases} \tag{3}$$

It should be noted that in the MATLAB implementation, the matrices B and B_d are merged into a single matrix, such that the state-space command ss can be used for simulation purposes.

The linearized dynamics (3) are then discretized using zero-order hold. The discrete-time state equation becomes:

$$x^+ = \Pi x + \Gamma u + \Gamma_d U_G \tag{4}$$

Here, $\Pi = e^{Ah}$, $\Gamma = \int_0^h e^{As} ds B$, $\Gamma_d = \int_0^h e^{As} ds B_d$, where h denotes the sampling time and A, B, B_d denote the state matrices in (3). A sampling time $h = 15$ min was chosen, which equals the sampling time in [8]. The discrete-time system formulation can easily be computed in MATLAB using the command c2d$(system, h)$, where *system* denotes the state-space description of the linearized model in which

the matrices B and B_d have been merged. By doing so, the following discrete-time system description was obtained:

$$\begin{cases} x^+ = \Pi x + \begin{bmatrix} \Gamma & \Gamma_d \end{bmatrix} \begin{bmatrix} u \\ U_G \end{bmatrix} \\ y = Cx + \begin{bmatrix} D & 0 \end{bmatrix} \begin{bmatrix} u \\ U_G \end{bmatrix} \end{cases} \tag{5}$$

It can be verified that all eigenvalues of Π lie strictly within the unit disk of the complex plane. Hence, the origin is an attractive equilibrium of the discrete-time system.

II. Model predictive control design

In this section, a model predictive control strategy is designed to safely regulate glucose peaks caused by meal intakes. To start, a state-measurement MPC algorithm is designed. This can be used to verify if performance specifications can be met. However, in general only the output y is measured. Hence, an observer will be added to the state-measurement MPC controller afterwards.

A. State-measurement MPC

A receding horizon MPC strategy is considered with control horizon $N = 6$. By doing so, the MPC controller will be able to notice upcoming disturbances in advance, while the computational complexity of the algorithm stays relatively low. Meal disturbances will be chosen, such that for this horizon length, the terminal set $\mathbb{X}_\mathrm{f}$ can be reached (i.e. $x(N) \in \mathbb{X}_\mathrm{f}$, assuming no additional disturbances are applied).

The states of the discretized system (5) are subject to different constraints. First of all, they must satisfy the system dynamics $x^+ = \Pi x + \begin{bmatrix} \Gamma & \Gamma_d \end{bmatrix} \begin{bmatrix} u \\ U_G \end{bmatrix}$, with $x(0) = 0$.

Furthermore, the states should be bounded to ensure safe glucose levels. Most importantly, the first state (Q_1) should be tightly bounded, as it directly impacts hyper- and hypoglycemia. Due to the loss of affine terms during linearization, physically relevant bounds proposed in [7] should be shifted, such that the steady-state glucose concentration lies at 0 mmol/L instead of 6 mmol/L. While output constraints could be used to achieve the shifted glucose level bound (i.e. $-2 \leq y(k) = Q_1(k)/V_G \leq 15$), we chose to formulate the output constraint as a constraint on Q_1. Loose constraints were added for other states, as these do not directly impact health, but should not go unbounded either.

The following state constraints have been obtained:

$$m = \begin{bmatrix} -0.4 \\ -2 \\ -100 \\ -50 \\ -50 \\ -0.5 \\ -1 \\ -4 \end{bmatrix} \leq \begin{bmatrix} Q_1(k) \\ Q_2(k) \\ S_1(k) \\ S_2(k) \\ I(k) \\ x_1(k) \\ x_2(k) \\ x_3(k) \end{bmatrix} \leq \begin{bmatrix} 2.4 \\ 2 \\ 250 \\ 150 \\ 150 \\ 1 \\ 1 \\ 10 \end{bmatrix} = M \tag{6}$$

The state constraints can now be represented compactly as $Fx(k) \leq e$, where F and e are given by:

$$F = \begin{bmatrix} I \\ -I \end{bmatrix}; \; e = \begin{bmatrix} M \\ -m \end{bmatrix}$$

Constraints are also put on the control action. For safety, only small insulin injections $u(k) \leq 6$ are allowed. As was discussed in Section I-B, small glucagon injections (negative inputs) are also allowed. It was decided that $u(k) \geq -2$. The input bounds can now be represented compactly as:

$$\begin{bmatrix} 1 \\ -1 \end{bmatrix} u(k) \leq \begin{bmatrix} 6 \\ 2 \end{bmatrix}$$

It should be noted that the optimal control problem may be unsolvable for some choices of the disturbance U_G, as all states and the control action are bounded. Hence, if a disturbance with a high glucose level D_G is supplied to the system, it may be possible that no feasible solution exists. Similarly, a terminal constraint $x(N) \in \mathbb{X}_\mathrm{f}$ will only be enforced after the disturbance U_G has reached its peak, as the dynamics of the system and the input constraints will destroy feasibility otherwise. It will be verified in the simulations of Section IV that these bounds work for a physically relevant range of disturbances U_G, with $D_G \in [0, 10]$ grams.

As a last step, cost functions were designed. The state cost function is given by $\ell(x, u) = \frac{1}{2}(x^T Q x + u^T R u)$, where $Q = diag(100, 1, 0.01, 0.01, 0.1, 1, 0.1, 1)$ and $R = 10$. The weights in Q were chosen, such that the state Q_1 is penalized harsly, states that directly influence Q_1 are penalized remotely harsh and states that indirectly influence Q_1 are penalized softly. R was chosen remotely high with respect to the entries of Q to limit the magnitude of the control action.

The terminal cost function was chosen as $V_f(x) = \frac{1}{2}x^T P x$, where P solves the discrete-time Lyapunov equation $A_K^T P A_K = P - 2Q_K$. Here, $A_K = \Pi + \Gamma K$ with K the solution to the discrete-time algebraic Riccati equation for the matrices (Π, Γ) and $Q_K = Q + K^T R K$. Furthermore, the ellipsoidal terminal set $\mathbb{X}_\mathrm{f} = \{x \in \mathbb{R}^8 | V_\mathrm{f}(x) \leq 10\}$ was chosen. In Section III, it will be shown that this terminal set is chosen appropriately, such that asymptotic stability of the origin of the closed-loop linear system can be proven.

To conclude, the optimal control problem can be compactly represented as:

$$\mathbb{P}_N(x_0, t) : \begin{cases} \min_{\mathbf{u_N}} & V_N(x_0, \mathbf{u_N}) \\ \text{s.t.} & x^+ = \Pi x + \begin{bmatrix} \Gamma & \Gamma_d \end{bmatrix} \begin{bmatrix} u \\ U_G \end{bmatrix} \\ & Fx(k) \leq e \\ & \begin{bmatrix} 1 \\ -1 \end{bmatrix} u(k) \leq \begin{bmatrix} 6 \\ 2 \end{bmatrix} \\ & x(N) \in \mathbb{X}_\mathrm{f} \text{ (if } U_G \text{ decreases)} \end{cases} \tag{7}$$

B. Output-measurement MPC

In practice, full state-measurements are unavailable. However, as (Π, C) is an observable pair, the states can be reconstructed using a state observer. The state-equation of the observer is given by (note again that the disturbance under consideration is assumed to be known):

$$\hat{x}^+ = (\Pi - LC)\hat{x} + \begin{bmatrix} \Gamma & \Gamma_d \end{bmatrix} \begin{bmatrix} u \\ U_G \end{bmatrix} + Ly \tag{8}$$

Here, the matrix L is chosen to be the Kalman observer gain with weighting matrices

$Q = diag(100, 1, 0.01, 0.01, 0.1, 1, 0.1, 1)$ and $R = 10$. As a result, $(\Pi - LC)$ has all its poles strictly within the unit disk in the complex plane, which means the error dynamics are asymptotically stable.

The MPC design of Section II-A stays intact for the output-measurement case, although the state x that is used in the design should be replaced by the observer state $\hat{x}$.

III. Asymptotic stability

In this section, we show that the MPC strategy proposed in Section II results in an asymptotically stable origin of the closed-loop linear system (5). It is assumed that the optimal control problem (7) is feasible. Moreover, it is assumed that a finite-in-time disturbance pattern is applied to the system, such that $U_G \to 0$ if $t \to \infty$. As a result, stability needs to be proven for a regulation task. This is a reasonable assumption, as if meal disturbances persist over time, the system would repeatedly be kicked out of its equilibrium position.

We will follow the approach of Section 2.5.3.1 of the book [10], which will ultimately result in the statement that Theorem 2.24(b) of [10] can be used to show that the origin of the linear system (5) is asymptotically stable. It will be verified by simulations in Section IV that the proposed MPC strategy is able to stabilize the continuous-time nonlinear system, but as this is not the main goal of the paper and as significant model adaptations have been made to arrive at the linear system (5), stability for the nonlinear system will not be proven.

A. Auxiliary results

Before any assumptions are verified, two auxiliary results are needed. These are:

1) $\mathbb{X}_\mathrm{f} \subseteq \mathbb{X}$
2) $K\mathbb{X}_\mathrm{f} \subseteq \mathbb{U}$

We now prove result (1) holds. Suppose $x \in \mathbb{X}_\mathrm{f}$ arbitrary. Then $x^T P x \leq 10$. Note that $\mathbb{X} = \{x \in \mathbb{R}^8 | m \leq x \leq M\}$ as proposed in Section II describes a hyperrectangular set. Note furthermore that $P \succ 0$ (i.e. P is symmetric and positive definite, or SPD), but that P is not necessarily a diagonal matrix. Hence, the ellipse described by $x^T P x \leq 10$ may be rotated with respect to axes of the coordinate system x, which makes it hard to show that $x \in \mathbb{X}$. To solve this problem, we aim to follow a procedure as illustrated in Figure 1 for $\mathbb{R}^2$.

As P is SPD, it is orthogonally diagonalizable. That is, $P = SDS^T$, where D is a matrix containing the (strictly positive) eigenvalues of P on the diagonal and S is an orthogonal matrix containing the eigenvectors of P, with $S^{-1} = S^T$. The ellipsoid can thus be described by $x^T S D S^T x \leq 10$. We now introduce the coordinate transformation $x = Sy$. The ellipsoid can then be described by $y^T D y \leq 10$. As D is a diagonal matrix, this ellipsoid is equivalently described by $\sum_{i=1}^{8} D_{ii} y_i^2 \leq 10$. Note that this ellipsoid intersects its each of its main axes y_i at locations $\pm\sqrt{10/D_{ii}}$.

Furthermore, we can apply the coordinate transform to the feasible set $\mathbb{X}$, to find $\mathbb{X} = \{y \in \mathbb{R}^8 | m \leq Sy \leq M\}$. To check if the ellipsoid is within this set, we define a higher-dimensional rhombus (also called hyper-rhombohedron) that (loosely) outer bounds the ellipsoid. Note that $\mathbb{X}_\mathrm{f}$ must lie within a rhombus that is twice as large as the ellipse on its main axes, as illustrated in Figure 1 (if this is not the case, then the shape is not an ellipsoid). Furthermore, note that for a rhombus, the constraints are most easily violated on one of its vertices. Hence, to see if the rhombus is contained in $\mathbb{X}$, we only need to check if its vertices are within $\mathbb{X}$. This therefore results in eight conditions of the form $m \leq S\bar{y}_i \leq M$, where $\bar{y}_i$ is a vector with entry i equal to $\pm 2\sqrt{10/D_{ii}}$ and zeros elsewhere. If these constraints hold, the rhombus is a subset of $\mathbb{X}$. As $\mathbb{X}_\mathrm{f}$ is a subset of the rhombus, it must follow that $\mathbb{X}_\mathrm{f} \subseteq \mathbb{X}$.

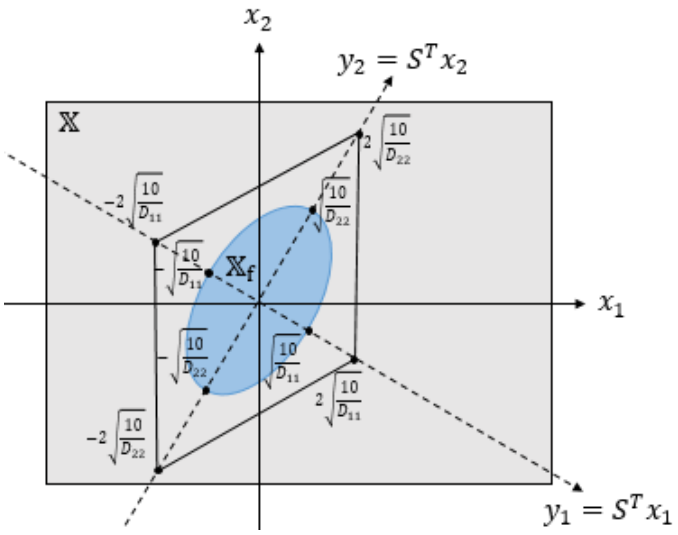

Fig. 1. Idea of the proofs of the auxiliary results for $\mathbb{R}^2$.

Using MATLAB, the vectors $S\bar{y}_i$ have been computed for $i \in \{1, 2, ..., 8\}$. We only need to look at the absolute largest value for each entry to determine if the bounds are violated. These are shown in the comparison below:

$$m = \begin{bmatrix} -0.4 \\ -2 \\ -100 \\ -50 \\ -50 \\ -0.5 \\ -1 \\ -4 \end{bmatrix} \leq \begin{bmatrix} \pm 0.34 \\ \pm 1.7 \\ \pm 38 \\ \pm 11.2 \\ \pm 13.8 \\ \pm 0.06 \\ \pm 0.34 \\ \pm 3.4 \end{bmatrix} \leq \begin{bmatrix} 2.4 \\ 2 \\ 250 \\ 150 \\ 150 \\ 1 \\ 1 \\ 10 \end{bmatrix} = M$$

It can be seen that the condition $m \leq S\bar{y}_i \leq M$ holds. Hence, it can be concluded that $\mathbb{X}_\mathrm{f} \subseteq \mathbb{X}$.

We now prove result (2) holds. Suppose $u \in K\mathbb{X}_\mathrm{f}$ arbitrary. Then $u = Kx$ with $x^T P x \leq 10$. By introducing the coordinate transform $x = Sy$ from the previous proof, this can equivalently be posed as $u = KSy$ with $y^T D y \leq 10$. Note that u has been formulated as a function of y, which means a similar proof as before can be used. The ellipsoid $y^T D y \leq 10$ can be rewritten as $\sum_{i=1}^{8} D_{ii} y_i^2 \leq 10$. As before, we check if a rhombus, twice as large as the ellipsoid on its main axes, does not violate the input bounds. By the reasoning introduced in the previous proof, this can be done by verifying eight conditions of the form $-2 \leq KS\bar{y}_i \leq 6$, where $\bar{y}_i$ is a vector with entry i equal to $\pm 2\sqrt{10/D_{ii}}$ and zeros elsewhere.

If these conditions on the vertices of the rhombus hold, then if x is in the rhombus, $Kx \in \mathbb{U}$. As the rhombus is an outer bound for the ellipsoid, it then follows that $K\mathbb{X}_\mathrm{f} \subseteq \mathbb{U}$.

Using MATLAB, the scalars $KS\bar{y}_i$ have been computed for all $i \in \{1, 2, ..., 8\}$. The absolute largest value of those scalars determines if the bounds are violated. This results in the following comparison:

$$-2 \leq \pm 1.08 \leq 6$$

Clearly, these conditions hold. Hence, it can be concluded that $K\mathbb{X}_\mathrm{f} \subseteq \mathbb{U}$.

B. Assumption 2.2

We now prove the assumptions underlying Theorem 2.24(b) of [10]. We recall from Section II that $\ell(x, u)$ and $V_f(x)$ are continuous, positive definite functions, as they are quadratic functions with $Q, R, P \succ 0$. Furthermore, the system description of Equation (5) is linear, which means it is continuous and has an equilibrium point at $(x, u) = (0, 0)$. Hence, Assumption 2.2 of [10] is satisfied.

C. Assumption 2.3

To verify if Assumption 2.3 of [10] holds, we recall from Section II that all states x and the control action u have been upper and lower bounded through non-strict inequalities. Similarly, the terminal set $\mathbb{X}_\mathrm{f}$ is bounded through a non-strict inequality $x^T P x \leq 10$. By auxiliary result (1), it follows that $\mathbb{X}_\mathrm{f} \subseteq \mathbb{X}$. It can thus be concluded that $\mathbb{X}$ is a closed set (as the boundary is included in the set) and that both $\mathbb{X}_\mathrm{f}$ and $\mathbb{U}$ are closed and bounded sets. By the Heine-Borel theorem, it can then be concluded that both $\mathbb{X}_\mathrm{f}$ and $\mathbb{U}$ are compact sets. Furthermore, as $\mathbb{X}_\mathrm{f}$ is an ellipsoidal level set around the origin, $0 \in \text{int}(\mathbb{X}_\mathrm{f})$ and $0 \in \text{int}(\mathbb{X})$ by set inclusion. By the constraints on $u(k)$, $0 \in \text{int}(\mathbb{U})$. We can conclude that Assumption 2.3 is satisfied.

D. Assumption 2.12

We now verify Assumptions 2.12 and 2.13 of [10]. For the system under consideration, these assumptions are verified if $\forall x \in \mathbb{X}_\mathrm{f}, \exists u \in \mathbb{U}$ s.t. $x^+ \in \mathbb{X}_\mathrm{f}$ and $V_f(x^+) \leq V_f(x) - \ell(x, u)$. That is, we should have control invariance and a Lyapunov decrease within the terminal set. By auxiliary results (1) and (2), we find that the control action $u = Kx$ satisfies the state- and input constraints if $x \in \mathbb{X}_\mathrm{f}$. That is,
$\mathbb{X}_\mathrm{f} \subseteq \{x \in \mathbb{X} | u = Kx \in \mathbb{U}\}$. Hence, we show these assumptions are satisfied for $u = Kx$.

For Assumption 2.12, it needs to be shown that
$V_f(\Pi x + \Gamma u + \Gamma_d U_G) \leq V_f(x) + \ell(x, u)$ for all $x \in \mathbb{X}_\mathrm{f}$. With $u = Kx$, $U_G \to 0$ and with the notation introduced in Section II, this reduces to $V_f(A_K x) \leq V_f(x) + \frac{1}{2} x^T Q_K x$. Note that $V_f(A_K x) = \frac{1}{2}(A_K x)^T P (A_k x) = \frac{1}{2} x^T A_K^T P A_K x$. As P solves the equation $A_K^T P A_K = P - 2Q_K$ (see Section II-A), we have (using $Q \succ 0$):

$$V_f(A_K x) = \frac{1}{2} x^T P x - x^T Q x$$

$$\leq \frac{1}{2} x^T P x - \frac{1}{2} x^T Q x = V_f(x) - \ell(x, u)$$

This means Assumption 2.12 is satisfied.

E. Assumption 2.13

For Assumption 2.13, we need to prove positive invariance of the terminal set for the chosen (and admissible) control action $u = Kx$. As $V_f(x) = \frac{1}{2} x^T P x$ with P the solution to the discrete algebraic Riccati equation, it follows that $V_f(x) = V_\infty^{unc}(x)$ (i.e. the optimal infinite horizon unconstrained cost function). For any finite horizon N, we have for the unconstrained optimal control problem:

$$V_N^{unc} = \min_{\mathbf{u}_N \in \mathbb{R}^{8N}} V_N(x, \mathbf{u}_N)$$

$$= \min_{\mathbf{u}_N \in \mathbb{R}^{8N}} \{ \sum_{k=0}^{N-1} \{\ell(x(k), u_N(k))\} + \frac{1}{2} x(N)^T P x(N) \}$$

Note that $\frac{1}{2} x(N)^T P x(N) = V_\infty^{unc}(x(N))$ (the optimal cost-to-go defined earlier). Furthermore, note that by the Bellman optimality principle, which (roughly speaking) states that any piece of optimal trajectory is optimal, we can rewrite the expression as:

$$V_N^{unc} = V_N^{unc}(x(0)) + V_\infty^{unc}(x(N))$$

$$= V_\infty^{unc}(x) = V_f(x)$$

Now, constraints are added to the problem. By adding constraints, limitations are added, which means there is less freedom in the optimization. As a result, the constrained optimal control cost will be higher. That is, $V_N^{unc} = V_f(x) \leq V_N^0(x), \forall x \in \mathcal{X}_N \supseteq \mathbb{X}_\mathrm{f}$, where $V_N^0(x)$ denotes the constrained optimal cost. By Lemma 2.15 of [10] (Monotonicity of the optimal value function), we also find that $V_N^0 \leq V_f(x), \forall x \in \mathbb{X}_\mathrm{f}$. We can thus conclude:

$$V_N^{unc}(x) = V_N^0(x) = V_f(x) = V_\infty^{unc}, \forall x \in \mathbb{X}_\mathrm{f}$$

As the solution to the optimal control problem is unique, it follows that:

$$\kappa_N(x) = \kappa_\infty^{unc}(x) = Kx, \forall x \in \mathbb{X}_\mathrm{f}$$

Therefore, $\mathbb{X}_\mathrm{f}$ is positive invariant for $x^+ = \Pi x + \Gamma \kappa_N(x) + \Gamma_d U_G$ if $U_G \to 0$ and positive invariance of $\mathbb{X}_\mathrm{f}$ under the control law κ_N follows by the MPC design. This completes the proof for Assumption 2.13.

F. Assumption 2.16

The last assumption that needs to be verified is Assumption 2.16 of [10]. As $\ell(x, u) = \frac{1}{2}(x^T Q x + u^T R u)$ with $Q, R \succ 0$, it follows that $\ell(x, u) = \frac{1}{2}(x^T Q x + u^T R u) \geq \frac{1}{2} x^T Q x \geq \frac{1}{2} \lambda_{min}(Q) |x|^2 = c_1 |x|^a$, with $c_1 = \frac{1}{2} \lambda_{min}(Q)$ and $a = 2$. Furthermore, we have $V_f(x) = \frac{1}{2} x^T P x \leq \frac{1}{2} \lambda_{max}(P) |x|^2 = c_2 |x|^a$, with $c_2 = \frac{1}{2} \lambda_{max}(P)$ and $a = 2$ as before. As a result, Assumption 2.16(b) is satisfied. Moreover, this also applies that Assumption 2.16(a) holds, as the given functions are class $\mathcal{K}_\infty$ functions (because they are norm functions, they are 0 at the origin, strictly increasing and radially unbounded).

G. Theorem 2.24(b)

It was shown that Assumptions 2.2, 2.3, 2.12, 2.13 and 2.16(a-b) of [10] are satisfied (and recall that $0 \in \text{int}(\mathbb{X}_f)$, as shown in the verification of Assumption 2.3). Hence, by Theorem 2.24(b) of [10], the origin of the closed-loop linear system (5) is asymptotically stable (and even exponentially stable) with region of attraction $\mathcal{X}_N$ for the controlled system $x^+ = \Pi x + \Gamma \kappa_N(x) + \Gamma_d U_G$ (with $U_G \to 0$).

IV. Numerical simulations

In this section, simulations are carried out using the MPC design from Section II. First, simulations of the linearized model in the state-measurement case will be shown. The control inputs are saved and applied to the nonlinear model. The influence of the horizon length N and the weighting matrices Q and R will be researched as well. Next, simulations of the linearized model in the output-measurement case will be shown. As a final step, a PI-controller is implemented on the nonlinear model, to be compared with the MPC strategy. To solve the optimal control problem, the convex optimization package CVX was used in MATLAB 2018b.

A. State-measurement MPC

In this first simulation, the MPC problem is solved for the state-measurement case. A single disturbance, acting at $t_0 = 0$ min and with glucose mass $D_G = 10$ g, was used in this simulation. The resulting glucose level is found in Figure 2. Note that, due to the loss of affine terms during linearization, the equilibrium glucose level is at 0 mmol/L instead of 6 mmol/L. This will be compensated for in the nonlinear system simulation.

From Figure 2, it can be seen that the MPC controller is able to reject the meal disturbance properly, satisfying the bounds on the output and control input. The amplitude of the hyperglycematic phase is reduced from 22 mmol/L (in the no control case) to 10.5 mmol/L. Furthermore, due to the glucagon input, no significant phase of hypoglycemia is present in the output. Therefore, the MPC controller was designed successfully.

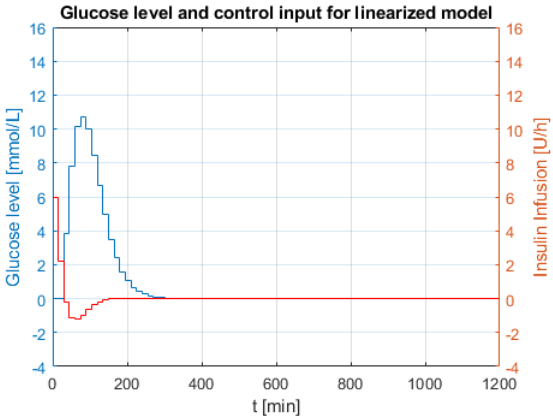

Fig. 2. Linearized model response and control input.

To further test the MPC control strategy, a second simulation for the linear system was carried out. In this simulation, three disturbances were used, arranged to represent a 3-meal structure of breakfast, lunch and dinner. For the breakfast disturbance, $t_0 = 0$ min and $D_G = 10$ g were used. For the lunch disturbance, $t_0 = 240$ min and $D_G = 10$ g were used. For the dinner disturbance, $t_0 = 600$ min and $D_G = 20$ g were used. To allow for feasible solutions with this disturbance pattern, the terminal constraint was relieved, to only act after the third disturbance had reached its peak value. The resulting response and control action can be found in Figure 3.

From Figure 3, it can be seen that the disturbances are rejected properly. The peaks in the phases of hyperglycemia are reduced by the control action. A large advantage of MPC becomes apparent in this figure: if the disturbance pattern is known in advance (i.e. if a patient indicates that a meal is coming up in 1.5 hours), the MPC controller can pre-compensate for the incoming meal disturbance by injecting insulin. In this way, a short, artificial phase of hypoglycemia can be created before a meal, such that the amplitude of the hyperglycematic phase is majorly reduced. This explains why the lunch disturbance has a smaller amplitude than the breakfast disturbance, even though the same glucose mass is ingested. It should be noted, however, that if a patient indicates that a meal is coming up and then not decides to eat, glucose levels will get dangerously low. This may be a reason to not use the designed MPC strategy.

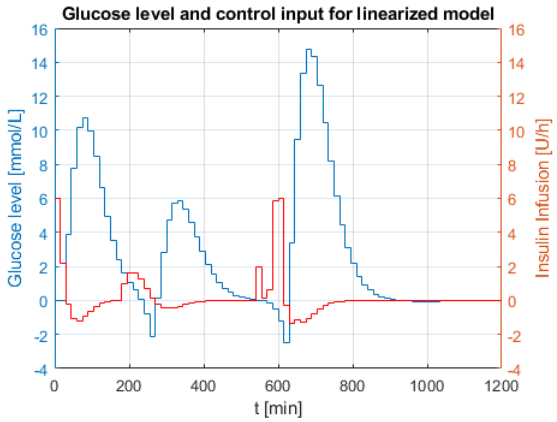

Fig. 3. Linearized model response and control input, 3 disturbance moments.

B. State-measurement control on nonlinear model

The control input sequences generated by the simulation of Section IV-A were applied to the nonlinear model of Equation (1), with a single disturbance acting at $t_0 = 0$ min with $D_G = 10$ g. To compensate for the affine terms that were lost due to linearization, a constant offset $u_c = 0.0185$ was added to the input sequence. That is, an input sequence $u = u_{lin} + u_c$ was supplied to the nonlinear model. This shifts the equilibrium value of 22.5 mmol/L (which is unsafe) to a safe equilibrium value of 6 mmol/L. The resulting intravenous glucose levels, with and without u_{lin}, are shown in Figure 4.

From Figure 4, it becomes apparent that the control sequence from the linearized model is able to significantly

reduce the hyperglycematic peak in the response. However, the hypoglycematic peak reaches a value of 1.2 mmol/L, which is highly dangerous, if not lethal. As expected, the control sequence generated by the linear model is too aggressive, due to the loss of the affine terms (which have a restorative effect) during linearization.

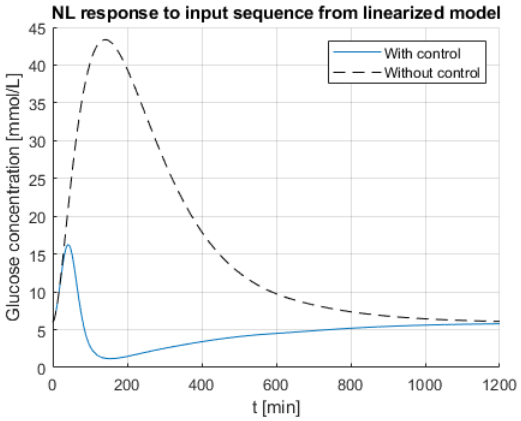

Fig. 4. Nonlinear model response to state-measurement input sequence.

While one could conclude that the control input sequence from the linear model is useless, due to the aggressiveness of the response, this is not necessarily true. It could be that the overall behavior of the control input is good, but that the magnitudes are too high. Hence, the control input generated by linear MPC is multiplied by a factor 0.35. The supplied control input is thus $\tilde{u} = 0.35u_{lin} + u_c$. The resulting intravenous glucose levels, with and without u_{lin}, are shown in Figure 5.

From Figure 5, it is seen that the hyperglycematic peak is still significantly reduced, with a peak value of 21.5 mmol/L. As this peak only persists for a short amount of time, it can be considered safe. Furthermore, the hypoglycematic peak reaches a value of 4.3 mmol/L, which is also safe. It can thus be said that the scaled input from linear MPC can be used successfully on the nonlinear model, with a satisfactory response. Furthermore, it has been verified that the input scale factor 0.35 gives satisfactory responses for $D_G \in \{0, 5, 10\}$ g. Hence, it can be assumed that this scaling factor can be used to scale linear MPC input sequences for $D_G \in [0, 10]$ grams.

C. Effect of horizon and weighting matrices

To research the effect of the horizon length N, the simulation of the linearized model with a single disturbance, acting at $t_0 = 0$ min with $D_G = 10$ g, was repeated for different horizon lengths. It was found that for $N \leq 2$, the constraints on the states and input could no longer be satisfied. This makes sense, as the hyper- and hypoglycematic peaks may appear too late in the optimization routine to compensate for them if the horizon length is very small. Furthermore, if $N > 6$, the output and control action closely resemble those for $N = 6$. This also makes sense, as the horizon $N = 6$ makes sure that the hyper- and hypoglycematic peaks appear early enough in the process, so that they can be compensated for. A plot for $N = 3$ is shown in Figure 6.

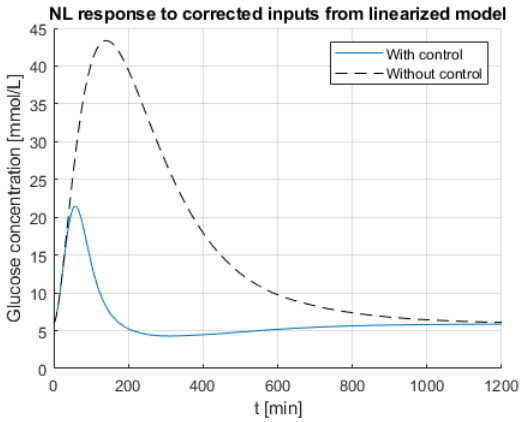

Fig. 5. Nonlinear model response to corrected state-measurement input sequence.

When Figure 6 is compared to Figure 2, it becomes apparent that the control inputs are smaller for $N = 3$, while the hyperglycematic peak is larger. This is a result of the fact that for $N = 3$, the hyper- and hypoglycematic peaks may appear too late to optimally compensate for them. As a result, small control inputs are chosen initially, as the MPC controller is not able to predict the amplitude of the disturbance.

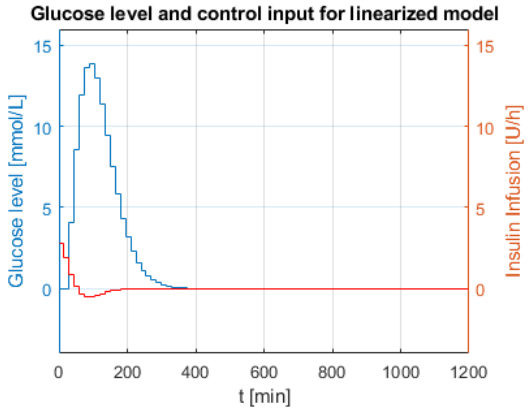

Fig. 6. Linearized model response for $N = 3$.

To research the effect of the weighting matrices Q and R on the outcome of the MPC control strategy, the simulation of the linearized model with a single disturbance, acting at $t_0 = 0$ min with $D_G = 10$ g, was repeated for the scaled weighting matrices $10 \cdot Q$ and $10 \cdot R$, separately. The resulting glucose levels and control inputs can be found in Figures 7 and 8, for the different weighting matrices respectively.

When Figure 7 is compared to Figure 2, it can be seen that the state-weighting matrix Q only has a small influence on the results. Increasing Q penalizes the state errors more heavily than the control action, which means that steering the states to zero becomes more important in the optimization. Hence, the disturbance amplitude has decreased somewhat, while the control input has increased. However, the effect is only marginal for the chosen matrices Q and R.

When Figure 8 is compared to Figure 2, it can be seen that the input-weighting matrix R has a significant influence

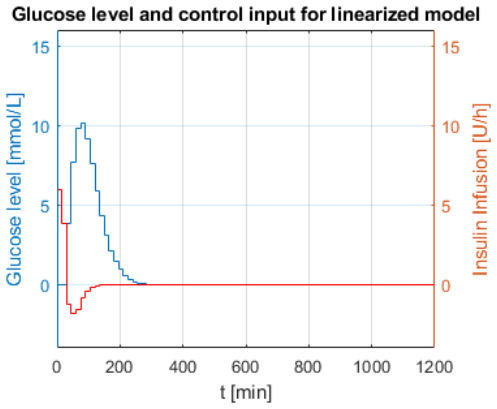

Fig. 7. Linearized model response for state-weight $10Q$.

on the results. Increasing R penalizes the control action more heavily than the state errors, which means that using small control actions becomes more important in the optimization. Hence, the disturbance amplitude has increased, while the control input has decreased.

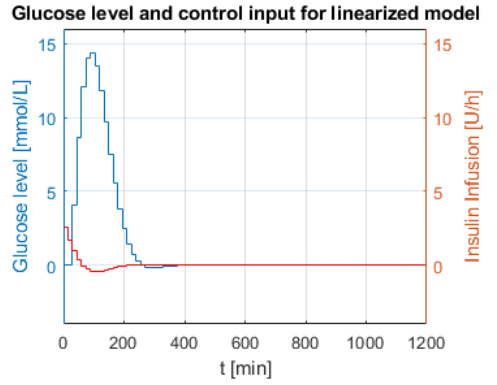

Fig. 8. Linearized model response for input-weight $10R$.

D. Output-measurement MPC

As full state-measurements are generally not available in this application, an observer was added to the MPC control scheme, as was described in Section II-B. For this control setup, the two simulations of Section IV-A have been carried out, with the system state being initialized at $x(0) = [0.7, 0.2, 2, 2, 5, 0.00065, 0.0009, 0.03]^T$. The results are found in Figures 9 and 10, respectively.

From these Figures, it can be concluded that the observer is able to quickly estimate the true state of the system. In the beginning, the control inputs are slightly higher when compared to Figures 2 and 3, as the observer needs to compensate for the non-optimal control actions that are applied to the system. Within 12 simulation steps, the difference between the observer state and the true state are marginal. From this point onwards, the glucose level and control action closely resemble the state-measurement case.

The generated input sequences have also been implemented on the nonlinear model, in a similar way as was done in Section IV-B. As the input sequences have only changed

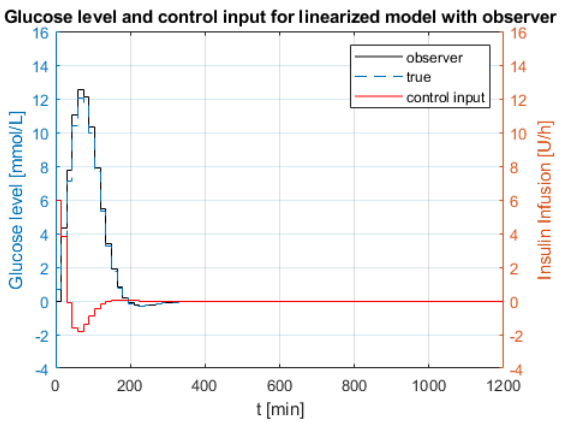

Fig. 9. Response and input for linearized model with observer.

slightly due to the introduction of the observer, the generated plots look similar to Figures 4 (no correction) and 5 (with correction), with slightly smaller hyper- and hypoglycematic peaks due to the increased control action.

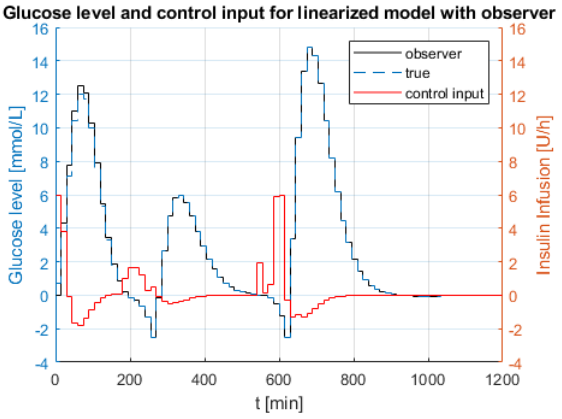

Fig. 10. Response and input for linearized model with observer, 3 disturbance moments.

E. Comparison with PI-control

A PI-controller was implemented on the nonlinear model, for comparison with the MPC results. The used PI-controller is given by:

$$K(s) = 0.02 + \frac{0.0001}{s}$$

The resulting glucose level and control action are found in Figure 11.

From Figure 10, it can be seen that the hyperglycematic peak (40 mmol/L) is only reduced somewhat with respect to the no-control case (43 mmol/L). Furthermore, the hypoglycematic phase takes more than 900 minutes, with a dangerous (or even lethal) hypoglycematic peak of 1.3 mmol/L. Clearly, this PI-controller is not able to reject the disturbance properly.

A possible reason for this bad behavior, is that the PI-controller is hindered by the time delay that is inherent to the system. Actions issued by the PI-controller start to affect the glucose level only after approximately 15 minutes. At this

time, the control action is no longer relevant. Furthermore, the controller has to have small gains. If the proportional gain is increased, sustained oscillations become apparent in the output as a result of the time delay. If the integral gain is increased, the system may even go unstable. Hence, MPC is preferred over PI-control.

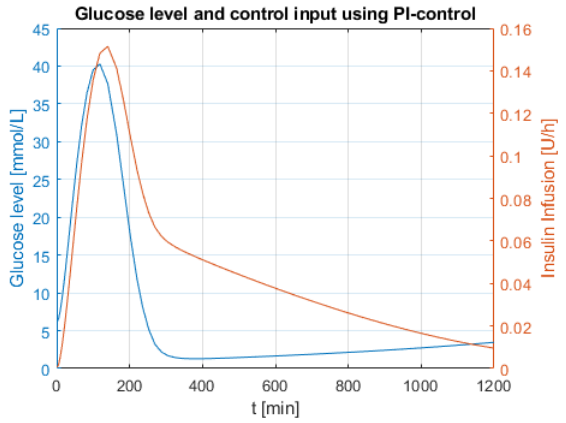

Fig. 11. Nonlinear model response and input for PI-controller.

V. Conclusion

In this paper, a linear model predictive control (MPC) strategy has been discussed, which can be used to reject meal disturbances in type 1 diabetes patients. Meal disturbances are generally characterized by a period of high glucose concentrations (hyperglycemia), followed by a period of low glucose concentrations (hypoglycemia). For type 1 diabetes patients, these effects are amplified, which makes control of meal disturbances important.

A nonlinear model describing the glucoregulatory system was described. This model was then linearized and discretized. For this discrete-time linear model, a MPC strategy was formulated. It was shown that asymptotic stability of the origin of the closed-loop linear system could be guaranteed for this strategy.

Through simulation, it has been shown that the linear MPC strategy is able to reject meal disturbances properly. By using a scaled version of this linear input, to correct for linearization inaccuracy, meal disturbances are also rejected properly for the nonlinear system. The effects of the horizon length and the weighting matrices have been discussed. If only output-measurements are used, the MPC strategy can still be used to reject meal disturbances. Lastly, it was shown that a PI-controller is not able to reject the disturbance properly. It can thus be concluded that linear MPC is a promising control strategy for regulating intravenous glucose levels in type 1 diabetes patients.

Future research could focus on linear MPC for type 2 diabetes patients. While these patients also suffer from low insulin production, the dynamics of the glucoregulatory system are different from the dynamics of Equation (1) [11]. Finding out if the proposed MPC strategy, or any other linear MPC strategy, can be used for these patients is an important research subject.

References

[1] D. Daneman, "Type 1 diabetes", *The Lancet*, vol. 367, no. 9513, pp. 847-858, 2006.

[2] M. Atkinson, G. Eisenbarth and A. Michels, "Type 1 diabetes", *The Lancet*, vol. 383, no. 9911, pp. 69-82, 2014.

[3] W. Tamborlane et al., "Continuous Glucose Monitoring and Intensive Treatment of Type 1 Diabetes", *New England Journal of Medicine*, vol. 359, no. 14, pp. 1464-1476, 2008.

[4] P. Li, L. Yu, L. Guo, J. Dong, J. Hu and Q. Fang, "PID control of glucose concentration in subjects with type 1 diabetes based on a simplified model: An in silico trial", *Proceedings of the 10th World Congress on Intelligent Control and Automation*, 2012.

[5] C. Li and R. Hu, "Fuzzy-PID Control for the Regulation of Blood Glucose in Diabetes", *2009 WRI Global Congress on Intelligent Systems*, 2009.

[6] G. Marchetti, M. Barolo, L. Jovanovic, H. Zisser and D. Seborg, "An Improved PID Switching Control Strategy for Type 1 Diabetes", *IEEE Transactions on Biomedical Engineering*, vol. 55, no. 3, pp. 857-865, 2008.

[7] R. Hovorka et al., "Partitioning glucose distribution/transport, disposal, and endogenous production during IVGTT", *American Journal of Physiology-Endocrinology and Metabolism*, vol. 282, no. 5, pp. E992-E1007, 2002.

[8] R. Hovorka et al., "Nonlinear model predictive control of glucose concentration in subjects with type 1 diabetes", *Physiological Measurement*, vol. 25, no. 4, pp. 905-920, 2004.

[9] A. Emami, J. Youssef, R. Rabasa-Lhoret, J. Pineau, J. Castle and A. Haidar, "Modeling Glucagon Action in Patients With Type 1 Diabetes", *IEEE Journal of Biomedical and Health Informatics*, vol. 21, no. 4, pp. 1163-1171, 2017.

[10] J. Rawlings and D. Mayne, *Model Predictive Control: Theory and Design*, 5th ed. Madison: Nob Hill Publishing, 2015.

[11] F. Nani and M. Jin, "Mathematical modeling and simulations of the pathophysiology of Type-2 Diabetes Mellitus", *2015 8th International Conference on Biomedical Engineering and Informatics (BMEI)*, 2015.